

Electromagnetic Scattering from One Dimensional Random Rough Surfaces of Dielectric Layered Media with Waveguide Modes Using Second Order Small Perturbation Method

Mohammadreza Sanamzadeh^{1, *}, Leung Tsang¹, Joel Johnson²,
Robert Burkholder², and Shurun Tan¹

Abstract—An alternative formulation of the Small Perturbation Method (SPM) in solving electromagnetic scattering from multi-layer random rough surfaces to resolve singularities in spectral integrals is presented. Non-monotonic permittivity changes will allow a multi-layer structure to support guided modes. The presence of these guided modes translates to poles in the zeroth order Green's function of the media for the surface fields. The poles appear in the first and second order perturbation solutions based on an iterative procedure. Thus, evaluating the spectral integrals to obtain the spatial fields becomes problematic. The Sommerfeld integration path instead of real line integrals is introduced by analytic continuation of the integrand into complex spectral space. It is verified that this alternative spectral integration method is valid for both monotonic and non-monotonic cases.

1. INTRODUCTION

The small perturbation method has been studied for random rough surface scattering extensively [1–12]. Recently, the method has been studied for multi-layered random rough surfaces [2, 5, 7] as an analytical method which has advantages over numerical methods for multiple rough interfaces. As the number of layers increases, numerical methods become costly in CPU and memory. An application of the multi-layered medium is microwave remote sensing of ice sheets in the Arctic and Antarctica, where the snow layers have multi-layering of fluctuations of permittivity due to the snow accumulation patterns as well as rough interfaces between layers [13].

The small perturbation method must be carried out to the second order [5] for energy conservation in emissivity calculations. In carrying out the Small Perturbation Method, the higher order field is expressed in terms of a convolution of the layered medium Green's function with the lower order field, where the convolution is performed in the spectral domain. To calculate the emissivity, the energy is decomposed into the incoherent intensity and the coherent intensity followed by the spectral integration. In the incoherent intensity, integration is to be carried out over the visible radiation spectrum. However, in the coherent intensity, integration is to be carried out over the entire k domain spectrum. In the case of a 1D rough surface with z as the vertical direction and x the horizontal direction (symmetry along y direction), the spectral domain integrations that appear in the coherent and incoherent intensities are continuous integrals over k_x . However, in a layered dielectric structure, when a dielectric layer has higher dielectric constant than its surrounding media, discrete waveguide modes exist. Mathematically, the waveguide modes correspond to the poles in the Green's function, and lie on the real k_x axis or close to the real k_x axis for lossless and slightly lossy dielectric, respectively. In a multi-layered medium,

Received 10 October 2017, Accepted 12 February 2018, Scheduled 19 February 2018

* Corresponding author: Mohammadreza Sanamzadeh (mrsanam@umich.edu).

¹ Department of Electrical Engineering and Computer Science, The University of Michigan, 1301 Beal Avenue, Ann Arbor, Michigan 48109, USA. ² Department of Electrical and Computer Engineering, The Ohio State University, 2015 Neil Avenue, Columbus, Ohio 43210, USA.

it also becomes difficult to determine the location of these poles to set up an appropriate numerical integration grid. The existence of waveguide modes presents a difficulty for the implementation of the second order small perturbation method.

The case of waveguide modes in layered media has been addressed in the past for higher orders of interaction [14–16]. In [14, 16], authors show that the waveguide modes can appear in the propagating part of the spectrum (Satellite Peaks) as a results of higher order of surface interaction. However, in second order perturbation waveguide poles are located in the evanescent part of the spectrum. In the case of random permittivity profile, when SPM2 solution always has such singularities, we present a numerical approach to resolve the case of singular integrand appearing in power calculations of SPM2.

In this paper, we consider the second order small perturbation method for a layered geometry when the permittivity profile allows the existence of waveguide modes. Our proposed solution is analytical continuation of the integrands to the complex plane and use the Sommerfeld integration path (SIP) to avoid possible poles on the real k_x axis. Another advantage of using the SIP is that the pole locations do not need to be known to perform the integrations. The SIP is applied to the cases of lossy dielectrics, monotonic permittivity profiles, and permittivity profiles which support guided modes to show its robustness. It is also shown that the use of the Sommerfeld path presents no additional increase in CPU time versus integration over the real k_x axis. We also compare the results with the T -matrix (Extended Boundary Condition) method [17] showing good agreement between our SPM2 alternative and the T -matrix method. The good agreement confirms the correctness of the method of the SIP in the presence of guided modes. The outline of the paper is as follows: In Section 2, the formulation of SPM2 for a two layered media with random rough interfaces is derived in details using compact operator notations. This will help to explain the origin of the main problem which is singular behavior of SPM2 kernel functions. Then, we briefly discuss obtaining scattered field and scattered power in terms of surface fields. In Section 4 the origin of pole singularities will be identified and an appropriate alternative path is introduced. Section 5 is dedicated to compare the SIP alternative to the T -matrix method. In the last section, comparison of the SIP alternative and the T -matrix method is given for the case of arbitrary number of layers with non-monotonic permittivity changes.

2. PROBLEM FORMULATION

The small perturbation solution for the scattering of electromagnetic waves from multi-layer media with rough interfaces has been studied in detail in [5]. Here we formulate the problem of a dielectric slab with two one-dimensional randomly rough surfaces, sandwiched between two semi-infinite dielectric media using a compact operator form which is more suitable for detection of the poles (Fig. 1). The formulation is based on the extinction theorem [18] and obtaining coupled surface integral equations for the surface fields on the interfaces. Application of the extinction theorem statement for region 0 in Fig. 1, results in

$$0 = \psi_i(k_x) - \frac{i}{2k_z} \left[A_0(k_x) - ik_z B_0(k_x) + \int dk'_x I_{00}^-(k_x, k'_x) \left\{ A_0(k'_x) - B_0(k'_x) i \frac{k^2 - k_x k'_x}{k_z} \right\} \right] \quad (1)$$

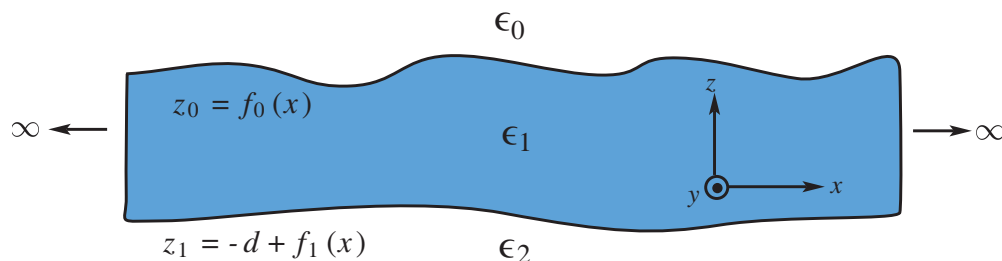


Figure 1. Geometry of the 2 layer problem with two random rough interfaces.

Here, $\psi_i(k_x)$ is the incident field ($\psi_i = E_{iy}$ and $\psi_i = H_{iy}$ for TE and TM polarizations, respectively) and $A(k_x)$ and $B(k_x)$ are spectral components of the surface magnetic and electric fields. On the first boundary, surface fields are defined as $a(x)dx = dl\hat{n} \cdot \nabla E_{0y}$ and $b(x) = E_{0y}(x)$ and related to the spectral fields by

$$\begin{aligned} a_0(x') &= \int dk'_x A_0(k'_x) e^{ik'_x x'} \\ b_0(x') &= \int dk'_x B_0(k'_x) e^{ik'_x x'} \end{aligned} \quad (2)$$

Also in Eq. (1), $I_{00}^-(k_x, k'_x)$ is the scattering potential due to the roughness of the first boundary described by $z = f_0(x)$ which is seen by downward propagating wave in the region 0 and is defined as

$$I_{00}^-(k_x, k'_x) = \frac{1}{2\pi} \int dx' e^{-i(k_x - k'_x)x'} \left[e^{ik_z f_0(x')} - 1 \right] \quad (3)$$

Similarly, defining the surface fields $a_1(x)$ and $b_1(x)$ on the other boundary characterized by $z = f_1(x) - d$ and then applying the extinction theorem to region 1 and region 2, we can write an integral equation describing all of the surface unknowns in the spectral domain as

$$\overline{\overline{G}}_0(k_x) \overline{\psi}(k_x) + \int dk'_x \overline{\overline{S}}(k_x, k'_x) \overline{\psi}(k'_x) = \overline{\psi}_i(k_x, k_{ix}) \quad (4)$$

Here $\overline{\psi}(k_x) = [A_0(k_x), B_0(k_x), A_1(k_x), B_1(k_x)]^T$ is the unknown surface field column vector and

$$\overline{\overline{G}}_0(k_x) = \begin{bmatrix} -\frac{i}{2k_z} & -\frac{1}{2} & 0 & 0 \\ \gamma_{01} & ik_{1z} & -e^{ik_{1z}d} & -ik_{1z}e^{ik_{1z}d} \\ \gamma_{01} & -ik_{1z} & -e^{-ik_{1z}d} & ik_{1z}e^{-ik_{1z}d} \\ 0 & 0 & \gamma_{12} & ik_{2z} \end{bmatrix} \quad (5)$$

is the propagator of the surface fields represented in the spectral domain corresponding to propagation of the fields inside the same layered media with flat interfaces. Also, the γ_{ij} 's are constant coefficients (coming from application of boundary conditions) which are $\gamma_{ij} = \mu_i/\mu_j$ and $\gamma_{ij} = \epsilon_i/\epsilon_j$ for TE and TM polarizations respectively. The presence of rough interfaces are described by the scattering operator $\overline{\overline{S}}(k_x, k'_x)$,

$$\overline{\overline{S}}(k_x, k'_x) = \begin{bmatrix} -\frac{i}{2k_z} I_{00}^-(k_x, k'_x) & -\frac{k^2 - k_x k'_x}{2k_z^2} I_{00}^-(k_x, k'_x) & 0 & 0 \\ \gamma_{01} I_{10}^+(k_x, k'_x) & i \frac{k_1^2 - k_x k'_x}{k_{1z}} I_{10}^+(k_x, k'_x) & -e^{ik_{1z}d} I_{11}^+(k_x, k'_x) & -e^{ik_{1z}d} i \frac{k_1^2 - k_x k'_x}{k_{1z}} I_{11}^+(k_x, k'_x) \\ \gamma_{01} I_{10}^-(k_x, k'_x) & -i \frac{k_1^2 - k_x k'_x}{k_{1z}} I_{10}^-(k_x, k'_x) & -e^{-ik_{1z}d} I_{11}^-(k_x, k'_x) & e^{-ik_{1z}d} i \frac{k_1^2 - k_x k'_x}{k_{1z}} I_{11}^-(k_x, k'_x) \\ 0 & 0 & \gamma_{12} I_{21}^+(k_x, k'_x) & i \frac{k_2^2 - k_x k'_x}{k_{2z}} I_{21}^+(k_x, k'_x) \end{bmatrix} \quad (6)$$

which is responsible for all orders of multiple scattering from each surface and also mutual interaction between the two boundaries. The scattering potentials $I_{mn}^\pm(k_x, k'_x)$ has the following form

$$I_{mn}^\pm(k_x, k'_x) = \frac{1}{2\pi} \int dx' e^{-i(k_x - k'_x)x'} \left[e^{\mp ik_{mz} f_n(x')} - 1 \right] \quad (7)$$

2.1. Perturbation Solution of Surface Field

In order to solve for the surface field $\overline{\psi}(k_x)$ we express it as a perturbation series

$$\overline{\psi}(k_x) = \overline{\psi}^{(0)}(k_x) + \overline{\psi}^{(1)}(k_x) + \overline{\psi}^{(2)}(k_x) + \dots \quad (8)$$

and then iterate solutions to find higher order surface fields.

2.1.1. Zeroth Order Solution

The zeroth order solution corresponds to the case of flat interfaces. The scattering potentials have been defined in such a way that they have no contribution to the zeroth order solution. In fact, if the waveguide modes exist for a particular configuration, they cannot be excited by an incident plane wave. Only a local source or perturbation such as a rough interface can excite the modes.

The scattering operator kernel is zero up to the zeroth order

$$\overline{\overline{S}}^{(0)}(k_x, k'_x) = \overline{0} \quad (9)$$

Thus, the zeroth order surface fields $\overline{\psi}^{(0)}(k_x)$ can be obtained easily from

$$\overline{\overline{G}}_0(k_x)\overline{\psi}^{(0)}(k_x) = \overline{\psi}_i(k_x, k_{ix}) = -\delta(k_x - k_{ix})[1 \ 0 \ 0 \ 0]^T \quad (10)$$

Since the right hand side is non zero only for $k_x = k_{ix}$, Equation (10) has a unique solution, if $|\overline{\overline{G}}_0(k_{ix})| \neq 0$

$$\overline{\psi}^{(0)}(k_x) = -\delta(k_x - k_{ix})\overline{\overline{G}}_0^{-1}(k_{ix})\overline{\psi}_i \quad (11)$$

Here we need to find how $|\overline{\overline{G}}_0(k_{ix})|$ behaves in order to examine the validity of solution (11). We will come back to this issue later in Section 4.

2.1.2. First Order Solution

Balancing the integral equation of the surface fields to the first order we have ($\overline{\overline{G}}_0$ is non-perturbative)

$$\overline{\overline{G}}_0(k_x)\overline{\psi}^{(1)}(k_x) + \int dk'_x \overline{\overline{S}}^{(1)}(k_x, k'_x)\overline{\psi}^{(0)}(k'_x) = 0 \quad (12)$$

Using the zeroth order solution we have

$$\overline{\overline{G}}_0(k_x)\overline{\psi}^{(1)}(k_x) - \overline{\overline{S}}^{(1)}(k_x, k_{ix})\overline{\overline{G}}_0^{-1}(k_{ix})\overline{\psi}_i = 0 \quad (13)$$

Now, if $|\overline{\overline{G}}_0(k_x)| \neq 0$ at a desired value of k_x , we can invert it to find

$$\overline{\psi}^{(1)}(k_x) = \overline{\overline{G}}_0^{-1}(k_x)\overline{\overline{S}}^{(1)}(k_x, k_{ix})\overline{\overline{G}}_0^{-1}(k_{ix})\overline{\psi}_i \quad (14)$$

However we will show that (see Section 4) at a resonance condition when the permittivity of the slab (ϵ_1) is larger than the surrounding medium ($\epsilon_0 < \epsilon_1 > \epsilon_2$), $\overline{\overline{G}}_0(k_x)$ is not invertible at the guided mode's cutoff frequency k_x^g , resulting in pole singularities in the spectral surface fields solution.

2.1.3. Second Order Solution

Balancing the integral equation of the surface fields to the second order results in

$$\overline{\overline{G}}_0(k_x)\overline{\psi}^{(2)}(k_x) + \int dk'_x \overline{\overline{S}}^{(2)}(k_x, k'_x)\overline{\psi}^{(0)}(k'_x) + \int dk'_x \overline{\overline{S}}^{(1)}(k_x, k'_x)\overline{\psi}^{(1)}(k'_x) = 0 \quad (15)$$

By substituting the zeroth order solution we have

$$\overline{\overline{G}}_0(k_x)\overline{\psi}^{(2)}(k_x) - \overline{\overline{S}}^{(2)}(k_x, k_{ix})\overline{\overline{G}}_0^{-1}(k_{ix})\overline{\psi}_i + \int dk'_x \overline{\overline{S}}^{(1)}(k_x, k'_x)\overline{\psi}^{(1)}(k'_x) = 0 \quad (16)$$

Now if $\overline{\overline{G}}_0(k_x)$ is invertible, we can solve for second order fields as

$$\overline{\psi}^{(2)}(k_x) = \overline{\overline{G}}_0^{-1}(k_x)\overline{\overline{S}}^{(2)}(k_x, k_{ix})\overline{\overline{G}}_0^{-1}(k_{ix})\overline{\psi}_i - \overline{\overline{G}}_0^{-1}(k_x) \int dk'_x \overline{\overline{S}}^{(1)}(k_x, k'_x)\overline{\psi}^{(1)}(k'_x) \quad (17)$$

Also substituting the first order surface fields of $\overline{\psi}^{(1)}(k_x)$, we obtain the second order solution as

$$\begin{aligned} \overline{\psi}^{(2)}(k_x) &= \overline{\overline{G}}_0^{-1}(k_x)\overline{\overline{S}}^{(2)}(k_x, k_{ix})\overline{\overline{G}}_0^{-1}(k_{ix})\overline{\psi}_i \\ &\quad - \overline{\overline{G}}_0^{-1}(k_x) \int dk'_x \overline{\overline{S}}^{(1)}(k_x, k'_x)\overline{\overline{G}}_0^{-1}(k'_x)\overline{\overline{S}}^{(1)}(k'_x, k_{ix})\overline{\overline{G}}_0^{-1}(k_{ix})\overline{\psi}_i \end{aligned} \quad (18)$$

3. SCATTERED AND TRANSMITTED FIELD

Using the spectral domain version of the equivalence principle applied to region 0 in Fig. 1, we can find the scattered field in region 0 as

$$\psi_s(k_x) = -\frac{i}{2k_z} \left[A_0(k_x) + ik_z B_0(k_x) + \int dk'_x I_{00}^+(k_x, k'_x) \left\{ A_0(k'_x) + B_0(k'_x) i \frac{k^2 - k_x k'_x}{k_z} \right\} \right] \quad (19)$$

Here, $\psi_s = E_{sy}$ and $\psi_s = H_{sy}$ for TE and TM polarizations, respectively. The surface fields solution $A_0(k_x)$ and $B_0(k_x)$ are known up to the second order from the extinction equations. The scattering potential due to roughness of the first boundary experienced by the upward going wave in region 0 is

$$I_{00}^+(k_x, k'_x) = \frac{1}{2\pi} \int dx' e^{-i(k_x - k'_x)x'} \left[e^{-ik_z f_0(x')} - 1 \right] \quad (20)$$

Similarly, the scattered field into region 2 (which is the transmitted field) can be obtained as

$$\psi_t(k_x) = \frac{i}{2k_{2z}} e^{-ik_{2z}d} \left[\gamma_{12} A_1(k_x) - ik_{2z} B_1(k_x) + \int dk'_x I_{21}^-(k_x, k'_x) \left\{ \gamma_{12} A_1(k'_x) - B_1(k'_x) i \frac{k_2^2 - k_x k'_x}{k_{2z}} \right\} \right] \quad (21)$$

in terms of surface fields $A_1(k_x)$ and $B_1(k_x)$ which are defined on the second boundary. $I_{21}^-(k_x, k'_x)$ is the potential due to roughness of the second surface experienced by the downward traveling wave in region 2 and is given by

$$I_{21}^-(k_x, k'_x) = \frac{1}{2\pi} \int dx' e^{-i(k_x - k'_x)x'} \left[e^{+ik_{2z} f_1(x')} - 1 \right] \quad (22)$$

If we define the scattered field column vector

$$\bar{\psi}_s(k_x) = \begin{bmatrix} \psi_s(k_x) \\ \psi_t(k_x) \end{bmatrix} \quad (23)$$

we can write relations in Eqs. (19) and (21) in a compact form

$$\bar{\psi}_s(k_x) = \bar{\bar{G}}_s^0(k_x) \bar{\psi}_s(k_x) + \int dk'_x \bar{\bar{S}}_s(k_x, k'_x) \bar{\psi}_s(k'_x) \quad (24)$$

where $\bar{\bar{G}}_s^0(k_x)$ is the propagator of the scattered field in the layered media with flat interfaces and is given by

$$\bar{\bar{G}}_s^0(k_x) = \begin{bmatrix} -\frac{i}{2k_z} & \frac{1}{2} & 0 & 0 \\ 0 & 0 & \frac{i}{2k_{2z}} e^{-ik_{2z}d} \gamma_{12} & \frac{1}{2} e^{-ik_{2z}d} \end{bmatrix} \quad (25)$$

$\bar{\bar{S}}_s(k_x, k'_x)$ is the scattering operator corresponding to the scattered field

$$\bar{\bar{S}}_s(k_x, k'_x) = \begin{bmatrix} -\frac{i}{2k_z} I_{00}^+(k_x, k'_x) & \frac{k^2 - k_x k'_x}{2k_z^2} I_{00}^+(k_x, k'_x) & & \\ & 0 & & \\ & & 0 & \\ & & & 0 \\ \frac{i}{2k_{2z}} e^{-ik_{2z}d} \gamma_{12} I_{21}^-(k_x, k'_x) & e^{-ik_{2z}d} \frac{k_2^2 - k_x k'_x}{2k_{2z}^2} I_{21}^-(k_x, k'_x) & & \end{bmatrix} \quad (26)$$

Now, we just need to insert the surface field solution into the governing relation of the scattered field in Eq. (24) to find different orders of scattered fields.

3.1. Zeroth Order Scattered Field

Balancing Eq. (24) up to the zeroth order, gives

$$\bar{\psi}_s^{(0)}(k_x) = \bar{\bar{G}}_s^0(k_x) \bar{\psi}_s^{(0)}(k_x) \quad (27)$$

Substituting the zeroth order solution of the surface fields in Eq. (11) into Eq. (27) results in

$$\bar{\psi}_s^{(0)}(k_x) = -\delta(k_x - k_{ix}) \bar{\bar{G}}_s^0(k_{ix}) \bar{\bar{G}}_0^{-1}(k_{ix}) \bar{\psi}_i \quad (28)$$

3.2. First Order Scattered Field

Up to the first order of perturbation, the scattered field is

$$\bar{\psi}_s^{(1)}(k_x) = \bar{G}_s^0(k_x) \bar{\psi}^{(1)}(k_x) + \int dk'_x \bar{S}_s^{(1)}(k_x, k'_x) \bar{\psi}^{(0)}(k'_x) \quad (29)$$

Using the zeroth and first order solution of the surface fields in Eqs. (11) and (14) we arrive at

$$\bar{\psi}_s^{(1)}(k_x) = \bar{G}_s^0(k_x) \bar{G}_0^{-1}(k_x) \bar{S}^{(1)}(k_x, k_{ix}) \bar{G}_0^{-1}(k_{ix}) \bar{\psi}_i - \bar{S}_s^{(1)}(k_x, k_{ix}) \bar{G}_0^{-1}(k_{ix}) \bar{\psi}_i \quad (30)$$

Now, we can split the scattering operators $\bar{S}^{(1)}$ and $\bar{S}_s^{(1)}$ into two parts, one corresponds to the effect of roughness due to the first boundary $\bar{S}_{F_0}^{(1)}$ and the other due to the presence of the second boundary $\bar{S}_{F_1}^{(1)}$. For $\bar{S}_s^{(1)}(k_x, k_{ix})$, we can write it as

$$\bar{S}_s^{(1)}(k_x, k_{ix}) = \bar{S}_{s,F_0}^{(1)}(k_x, k_{ix}) F_0(k_x - k_{ix}) + \bar{S}_{s,F_1}^{(1)}(k_x, k_{ix}) F_1(k_x - k_{ix}) \quad (31)$$

Here

$$\bar{S}_{s,F_0}^{(1)}(k_x, k_{ix}) = \begin{bmatrix} -\frac{1}{2} & -i \frac{k^2 - k_x k_{ix}}{2k_z} & 0 & 0 \\ 0 & 0 & 0 & 0 \end{bmatrix} \quad (32)$$

$$\bar{S}_{s,F_1}^{(1)}(k_x, k_{ix}) = \begin{bmatrix} 0 & 0 & 0 & 0 \\ 0 & 0 & -\frac{1}{2} e^{-ik_{2z}d} \gamma_{12} & e^{-ik_{2z}d} i \frac{k^2 - k_x k_{ix}}{2k_{2z}} \end{bmatrix} \quad (33)$$

and $F_j(k_x)$ is the Fourier Transform of the j -th surface boundary $f_j(x)$. Using this separation, we can divide the first order scattered field into contributions from each rough interface,

$$\bar{\psi}_s^{(1)}(k_x) = \bar{\psi}_{s,F_0}^{(1)}(k_x) F_0(k_x - k_{ix}) + \bar{\psi}_{s,F_1}^{(1)}(k_x) F_1(k_x - k_{ix}) \quad (34)$$

where

$$\bar{\psi}_{s,F_j}^{(1)}(k_x) = \left[\bar{G}_s^0(k_x) \bar{G}_0^{-1}(k_x) \bar{S}_{F_j}^{(1)}(k_x, k_{ix}) - \bar{S}_{s,F_j}^{(1)}(k_x, k_{ix}) \right] \bar{G}_0^{-1}(k_{ix}) \bar{\psi}_i, \quad j = 0, 1 \quad (35)$$

3.3. Second Order Scattered Field

Balancing Eq. (24) up to the second order of perturbation yields the second order scattered field in terms of different orders (0, 1, 2) of the surface field solution as

$$\bar{\psi}_s^{(2)}(k_x) = \bar{G}_s^0(k_x) \bar{\psi}^{(2)}(k_x) + \int dk'_x \bar{S}_s^{(2)}(k_x, k'_x) \bar{\psi}^{(0)}(k'_x) + \int dk'_x \bar{S}_s^{(1)}(k_x, k'_x) \bar{\psi}^{(1)}(k'_x) \quad (36)$$

Using the zeroth and first order surface fields solution of Eqs. (11) and (14) we have

$$\begin{aligned} \bar{\psi}_s^{(2)}(k_x) &= \bar{G}_s^0(k_x) \bar{\psi}^{(2)}(k_x) - \bar{S}_s^{(2)}(k_x, k_{ix}) \bar{G}_0^{-1}(k_{ix}) \bar{\psi}_i \\ &\quad + \int dk'_x \bar{S}_s^{(1)}(k_x, k'_x) \bar{G}_0^{-1}(k'_x) \bar{S}^{(1)}(k'_x, k_{ix}) \bar{G}_0^{-1}(k_{ix}) \bar{\psi}_i \end{aligned} \quad (37)$$

Similar to the decomposition of the first order scattering operator in Eq. (31), the second order scattering operator is written as

$$\bar{S}_s^{(2)}(k_x, k_{ix}) = \bar{S}_{s,F_0}^{(2)}(k_x, k_{ix}) F_0^{(2)}(k_x - k_{ix}) + \bar{S}_{s,F_1}^{(2)}(k_x, k_{ix}) F_1^{(2)}(k_x - k_{ix}) \quad (38)$$

$F_j^{(2)}(k_x - k_{ix})$ is the convolution of the j -th surface spectrum F_j with itself, which is evaluated at $k_x - k_{ix}$. The marginal second order scattering operators corresponding to the scattered field are given by

$$\overline{\overline{S}}_{s,F_0}^{(2)}(k_x, k_{ix}) = \frac{1}{2} \begin{bmatrix} ik_z & -\frac{k^2 - k_x k_{ix}}{2} & 0 & 0 \\ 2 & 0 & 0 & 0 \\ 0 & 0 & 0 & 0 \end{bmatrix} \quad (39)$$

$$\overline{\overline{S}}_{s,F_1}^{(2)}(k_x, k_{ix}) = \frac{1}{2} \begin{bmatrix} 0 & 0 & 0 & 0 \\ 0 & 0 & -\frac{ik_{2z}}{2} e^{-ik_{2z}d} \gamma_{12} & -e^{-ik_{2z}d} \frac{k_x^2 - k_x k_{ix}}{2} \end{bmatrix} \quad (40)$$

Thus, the second order scattered field becomes

$$\begin{aligned} \overline{\overline{\psi}}_s^{(2)}(k_x) &= \overline{\overline{G}}_s^0(k_x) \overline{\overline{\psi}}^{(2)}(k_x) - F_0^{(2)}(k_x - k_{ix}) \overline{\overline{S}}_{s,F_0}^{(2)}(k_x, k_{ix}) \overline{\overline{G}}_0^{-1}(k_{ix}) \overline{\overline{\psi}}_i \\ &\quad - F_1^{(2)}(k_x - k_{ix}) \overline{\overline{S}}_{s,F_1}^{(2)}(k_x, k_{ix}) \overline{\overline{G}}_0^{-1}(k_{ix}) \overline{\overline{\psi}}_i \\ &\quad + \int dk'_x F_0(k_x - k'_x) F_0(k'_x - k_{ix}) \overline{\overline{S}}_{s,F_0}^{(1)}(k_x, k'_x) \overline{\overline{G}}_0^{-1}(k'_x) \overline{\overline{S}}_{F_0}^{(1)}(k'_x, k_{ix}) \overline{\overline{G}}_0^{-1}(k_{ix}) \overline{\overline{\psi}}_i \\ &\quad + \int dk'_x F_0(k_x - k'_x) F_1(k'_x - k_{ix}) \overline{\overline{S}}_{s,F_0}^{(1)}(k_x, k'_x) \overline{\overline{G}}_0^{-1}(k'_x) \overline{\overline{S}}_{F_1}^{(1)}(k'_x, k_{ix}) \overline{\overline{G}}_0^{-1}(k_{ix}) \overline{\overline{\psi}}_i \\ &\quad + \int dk'_x F_1(k_x - k'_x) F_0(k'_x - k_{ix}) \overline{\overline{S}}_{s,F_1}^{(1)}(k_x, k'_x) \overline{\overline{G}}_0^{-1}(k'_x) \overline{\overline{S}}_{F_0}^{(1)}(k'_x, k_{ix}) \overline{\overline{G}}_0^{-1}(k_{ix}) \overline{\overline{\psi}}_i \\ &\quad + \int dk'_x F_1(k_x - k'_x) F_1(k'_x - k_{ix}) \overline{\overline{S}}_{s,F_1}^{(1)}(k_x, k'_x) \overline{\overline{G}}_0^{-1}(k'_x) \overline{\overline{S}}_{F_1}^{(1)}(k'_x, k_{ix}) \overline{\overline{G}}_0^{-1}(k_{ix}) \overline{\overline{\psi}}_i \end{aligned} \quad (41)$$

Before proceeding further, we take the statistical average of the scattered field. The mean field expression can be derived with less effort, since averaging of statistical expressions in the scattered field can be simplified greatly using

$$\begin{aligned} \langle F^{(2)}(k_x - k_{ix}) \rangle &= \delta(k_x - k_{ix}) \int dk'_x W(k'_x - k_{ix}) \\ \langle F(k_x - k'_x) F(k'_x - k_{ix}) \rangle &= \delta(k_x - k_{ix}) W(k'_x - k_{ix}) \end{aligned} \quad (42)$$

The only assumption made in deriving Eq. (42) is that the surface processes are assumed to be stationary. The second order spectral mean scattered field $\langle \overline{\overline{\psi}}_s^{(2)}(k_x) \rangle$ can be decomposed into linear contributions from each boundary, that is

$$\langle \overline{\overline{\psi}}_s^{(2)}(k_x) \rangle = \delta(k_x - k_{ix}) \int dk'_x \left[\langle \overline{\overline{\psi}}_s^{(2)} \rangle_{W_0} W_0(k'_x - k_{ix}) + \langle \overline{\overline{\psi}}_s^{(2)} \rangle_{W_1} W_1(k'_x - k_{ix}) \right] \quad (43)$$

where

$$\begin{aligned} \langle \overline{\overline{\psi}}_s^{(2)} \rangle_{W_0} &= \left\{ \overline{\overline{G}}_s^0(k_{ix}) \overline{\overline{G}}_0^{-1}(k_{ix}) \left[\overline{\overline{S}}_{F_0}^{(2)}(k_{ix}, k_{ix}) - \overline{\overline{S}}_{F_0}^{(1)}(k_{ix}, k'_x) \overline{\overline{G}}_0^{-1}(k'_x) \overline{\overline{S}}_{F_0}^{(1)}(k'_x, k_{ix}) \right] \right. \\ &\quad \left. - \overline{\overline{S}}_{s,F_0}^{(2)}(k_{ix}, k_{ix}) + \overline{\overline{S}}_{s,F_0}^{(1)}(k_{ix}, k'_x) \overline{\overline{G}}_0^{-1}(k'_x) \overline{\overline{S}}_{F_0}^{(1)}(k'_x, k_{ix}) \right\} \overline{\overline{G}}_0^{-1}(k_{ix}) \overline{\overline{\psi}}_i \end{aligned} \quad (44)$$

$$\begin{aligned} \langle \overline{\overline{\psi}}_s^{(2)} \rangle_{W_1} &= \left\{ \overline{\overline{G}}_s^0(k_{ix}) \overline{\overline{G}}_0^{-1}(k_{ix}) \left[\overline{\overline{S}}_{F_1}^{(2)}(k_{ix}, k_{ix}) - \overline{\overline{S}}_{F_1}^{(1)}(k_{ix}, k'_x) \overline{\overline{G}}_0^{-1}(k'_x) \overline{\overline{S}}_{F_1}^{(1)}(k'_x, k_{ix}) \right] \right. \\ &\quad \left. - \overline{\overline{S}}_{s,F_1}^{(2)}(k_{ix}, k_{ix}) + \overline{\overline{S}}_{s,F_1}^{(1)}(k_{ix}, k'_x) \overline{\overline{G}}_0^{-1}(k'_x) \overline{\overline{S}}_{F_1}^{(1)}(k'_x, k_{ix}) \right\} \overline{\overline{G}}_0^{-1}(k_{ix}) \overline{\overline{\psi}}_i \end{aligned} \quad (45)$$

Here we assume that the two surface processes $f_0(x)$ and $f_1(x)$ are uncorrelated.

3.4. Scattered and Transmitted Power

The scattered field in region 0 can be written in spatial coordinates as

$$\psi_s(\bar{r}) = \int dk_x \psi_s(k_x) e^{ik_x x + ik_z z} \quad (46)$$

For different orders of the scattered field we have

$$\psi_s^{(0)}(\bar{r}) = \psi_s^{(0)}(k_{ix}) e^{ik_{ix} x + ik_{iz} z} \quad (47)$$

$$\psi_s^{(1)}(\bar{r}) = \int dk_x e^{ik_x x + ik_z z} \left[\psi_{s,F_0}^{(1)}(k_x) F_0(k_x - k_{ix}) + \psi_{s,F_1}^{(1)}(k_x) F_1(k_x - k_{ix}) \right] \quad (48)$$

$$\langle \psi_s^{(2)}(\bar{r}) \rangle = e^{ik_{ix} x + ik_{iz} z} \int dk'_x \left[\langle \psi_s^{(2)} \rangle_{W_0} W_0(k'_x - k_{ix}) + \langle \psi_s^{(2)} \rangle_{W_1} W_1(k'_x - k_{ix}) \right] \quad (49)$$

Here $\psi_s = E_{sy}$ is the y -component of the electric field associated with the scattered wave for TE polarized incident field. The case of TM-polarized excitation can be obtained using duality principle. The mean scattered power density can be expressed in terms of the electric field as

$$\langle \bar{S}_s \cdot \hat{z} \rangle = -\frac{1}{2} \text{Im} \left[\frac{1}{k\eta} \left\langle E_{sy} \frac{\partial E_{sy}^*}{\partial z} \right\rangle \right] \quad (50)$$

Noting that the first order scattered field has zero mean, the coherent power density flowing upward can be written as

$$\langle \bar{S}_s \cdot \hat{z} \rangle_{\text{coh}} = \frac{1}{2} \text{Re} \left[\frac{k_{iz}}{k\eta} \left(|E_{sy}^{(0)}|^2 + 2 \langle E_{sy}^{(2)} \rangle E_{sy}^{(0)*} \right) \right] \quad (51)$$

then we can decompose the coherent scattered power into zeroth order and second order parts

$$\langle \bar{S}_s \cdot \hat{z} \rangle_{\text{coh}}^{(0)} = \frac{1}{2} \text{Re} \left[\frac{k_{iz}}{k\eta} |E_{sy}^{(0)}|^2 \right] \quad (52)$$

$$\langle \bar{S}_s \cdot \hat{z} \rangle_{\text{coh}}^{(2)} = \text{Re} \left[\frac{k_{iz}}{k\eta} \langle E_{sy}^{(2)} \rangle E_{sy}^{(0)*} \right] \quad (53)$$

The zeroth order scattered power is the power scattered by the same structure with flat boundaries. Using the second order mean scattered field in Eq. (43) we have the coherent mean power density in \hat{z} direction as

$$\begin{aligned} \langle \bar{S}_s \cdot \hat{z} \rangle_{\text{coh}}^{(2)} &= \int dk'_x \text{Re} \left[\frac{k_{iz}}{k\eta} \psi_s^{(0)*}(k_{ix}) \left[\langle \psi_s^{(2)} \rangle_{W_0} W_0(k'_x - k_{ix}) + \langle \psi_s^{(2)} \rangle_{W_1} W_1(k'_x - k_{ix}) \right] \right] \\ &= \sum_{j=0,1} \int dk'_x \Phi_{s,j}^{\text{coh}}(k'_x) W_j(k'_x - k_{ix}) \end{aligned} \quad (54)$$

where we call $\Phi_{s,j}^{\text{coh}}(k'_x)$, the j -th surface coherent scattered power spectral coefficient. The incoherent power originates from the first order scattered field

$$\langle \bar{S}_s \cdot \hat{z} \rangle_{\text{incoh}} = -\frac{1}{2} \text{Im} \left[\frac{1}{k\eta} \left\langle E_{sy}^{(1)} \frac{\partial E_{sy}^{(1)*}}{\partial z} \right\rangle \right] = \frac{1}{2} \text{Re} \left[\frac{k_z}{k\eta} \langle E_{sy}^{(1)} E_{sy}^{(1)*} \rangle \right] \quad (55)$$

However, assuming uncorrelated surface processes, we have

$$\langle \psi_s^{(1)}(\bar{r}) \psi_s^{(1)*}(\bar{r}) \rangle = \int dk_x \left[\left| \psi_{s,F_0}^{(1)}(k_x) \right|^2 W_0(k_x - k_{ix}) + \left| \psi_{s,F_1}^{(1)}(k_x) \right|^2 W_1(k_x - k_{ix}) \right] \quad (56)$$

Therefore, the incoherent power density flowing in the z direction can be written in terms of surface spectra

$$\langle \bar{S}_s \cdot \hat{z} \rangle_{\text{incoh}} = \frac{1}{2k\eta} \int dk_x \text{Re}(k_z) \left[\left| \psi_{s,F_0}^{(1)}(k_x) \right|^2 W_0(k_x - k_{ix}) + \left| \psi_{s,F_1}^{(1)}(k_x) \right|^2 W_1(k_x - k_{ix}) \right] \quad (57)$$

and the transmitted power can be computed similarly. The connection between the spectral and spatial representation of the transmitted field into region 2 is as follows

$$\psi_t(\bar{r}) = \int dk_x \psi_t(k_x) e^{ik_x x - ik_{2z} z} \quad (58)$$

Following the same procedure as the scattered field, we have similar expressions for the coherent and incoherent transmitted power densities along $(-\hat{z})$ direction

$$\langle \bar{S}_t \cdot \hat{z} \rangle_{\text{coh}}^{(2)} = \int dk'_x \text{Re} \left[\frac{k_{2iz}}{k_2 \eta_2} \psi_t^{(0)*}(k_{ix}) \left[\langle \psi_t^{(2)} \rangle_{W_0} W_0(k'_x - k_{ix}) + \langle \psi_t^{(2)} \rangle_{W_1} W_1(k'_x - k_{ix}) \right] \right] \quad (59)$$

$$\langle \bar{S}_t \cdot (-\hat{z}) \rangle_{\text{incoh}} = \frac{1}{2k\eta} \int dk_x \text{Re}(k_{2z}) \left[\left| \psi_{t,F_0}^{(1)}(k_x) \right|^2 W_0(k_x - k_{ix}) + \left| \psi_{t,F_1}^{(1)}(k_x) \right|^2 W_1(k_x - k_{ix}) \right] \quad (60)$$

4. WAVEGUIDE MODES AND SOMMERFELD INTEGRATION PATH

In the case of resonance condition, when $\epsilon_0 < \epsilon_1 > \epsilon_2$, layered media can support guided modes at specific spectral frequencies k_x^g for which $|\bar{G}_0(k_x^g)| = 0$. Surface field quantities which are governed by $\bar{G}_0(k_x)$, will have pole singularities at $k_x = k_x^g$. The determinant of the flat surface layered media propagator $\bar{G}_0(k_x)$ can be evaluated as

$$\left| \bar{G}_0(k_x) \right| = \frac{-i}{k_z} e^{-ik_{1z}d} (\gamma_{01}k_z + k_{1z})(\gamma_{12}k_{1z} + k_{2z}) \left[1 + R_{01}(k_x)R_{12}(k_x)e^{2ik_{1z}d} \right] \quad (61)$$

where $k_{jz}^2 + k_x^2 = k_j^2$ and

$$R_{01}(k_x) = \frac{\gamma_{01}k_z - k_{1z}}{\gamma_{01}k_z + k_{1z}} \quad (62)$$

$$R_{12}(k_x) = \frac{\gamma_{12}k_{1z} - k_{2z}}{\gamma_{12}k_{1z} + k_{2z}} \quad (63)$$

are electric field reflection coefficients from the two interfaces (assuming unbounded media). Also, $\gamma_{ij} = \epsilon_j/\epsilon_i$ for TM polarization and $\gamma_{ij} = \mu_j/\mu_i$ for a TE polarized wave. For simplicity, consider the case of TE polarized incident field and non-magnetic media. In this scenario, we do not have any depolarization and all of the field quantities preserve the incident polarization. In this case the determinant of $\bar{G}_0(k_x)$ becomes

$$\left| \bar{G}_0(k_x) \right| = \frac{-i}{k_z} e^{-ik_{1z}d} (k_z + k_{1z})(k_{1z} + k_{2z}) \left[1 + R_{01}(k_x)R_{12}(k_x)e^{2ik_{1z}d} \right] \quad (64)$$

The terms $(k_z + k_{1z})$ and $(k_{1z} + k_{2z})$ cannot be zero for distinct media (also, for the case of same media it will cancel out by the denominator). The only terms that can produce poles (eigenvalues of the propagator) comes from the expression

$$N(k_x) = 1 + R_{01}(k_x)R_{12}(k_x)e^{2ik_{1z}d} \quad (65)$$

For the lossless case and under guidance condition, $N(k_x)$ has real zeros at $k_x = k_x^g$ that will translate to real poles in the surface field solutions. These poles manifest themselves in both the first and second order surface fields.

In this situation, using the conventional definition of Fourier integrals to come back from spectral space to spatial space is illegal from a mathematical point of view. Computing the spectral integral over the real line contains only the principal value integral, and exact value of the integral is indefinite. Also from a physical point of view, singular behaviors should be investigated. On the other hand, a principal value integral has its own difficulties. First, we need to know the location of the poles which requires solving a nonlinear equation which is a time consuming task for real problems of random media with a large number of layers and ensemble of physical parameters, and second, when we know the poles' locations, it is necessary to use a dense numerical integration grid near the poles to capture the principal value integral correctly.

Instead of using spectral integrals over the real line, we will use the notion of analytic continuation of integrands and deform the path of integration into a Sommerfeld path alternative. This ensures definite values for the integrals and meaningful quantities in the spectral domain. Therefore we need to formulate the problem by changing spectral integrals as

$$\int_{\mathbb{R}} dk_x \implies \int_{\text{SIP}} dk_x \quad (66)$$

In order to find the correct perturbed path of integration, or the Sommerfeld path of integration (SIP), we need to insert a small amount of loss such that propagating waves satisfy the radiation condition at infinity correctly. Then as the loss tends to zero we can identify the correct path of integration. Note that the SIP should work for a small loss condition, so this is our selection rule. In Fig. 2, with a small amount of loss, poles reside in the first quadrant (and also in the third quadrant). So for the lossless case, poles in the first quadrant merge to the real axis from the upper half plane. So, the appropriate SIP is passing through the second and fourth quadrants. Note also that branch cuts (compatible with the radiation condition) for a lossy problem start from the poles in the upper half plane and converge to the real axis. By this selection we avoid crossing any branch cuts.

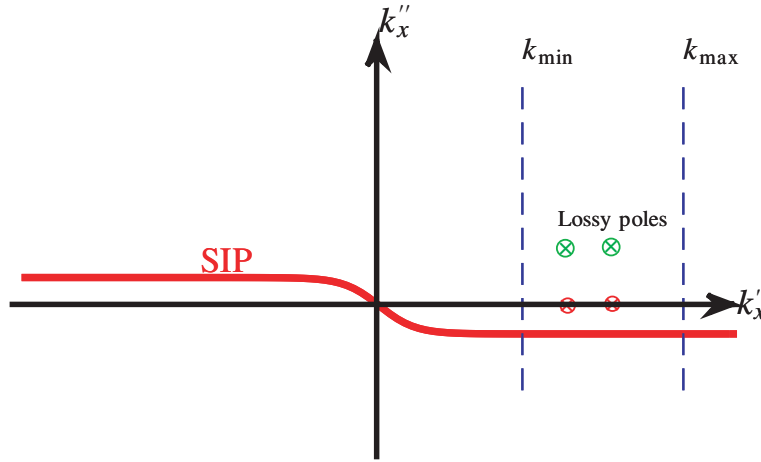


Figure 2. Appropriate Sommerfeld path of integration for the case of lossless layered dielectric media. SIP is chosen such that it does not pass over the poles or branch cuts of k_{jz} ($j = 0, 1, 2$).

4.1. Sommerfeld Integration Path: Numerical Examples

In order to illustrate the concept, consider the special case of two layered media with lossless materials given by $\epsilon_0 = \epsilon_0$, $\epsilon_1 = 4\epsilon_0$ and $\epsilon_2 = 2\epsilon_0$ with separation of layers $d = 0.7\lambda_0$ which can support a guided mode (λ_0 is free space wavelength). In this case we can find zeros of $N(k_x)$ numerically at $k_x = 1.684k_0$ and $k_x = 1.923k_0$. Both of the guided modes are evanescent in the z direction in the upper and lower regions. For incoherent scattered and transmitted intensities, the averaged propagating power density (real part of the poynting vector) of Equations (57) and (60) are limited to the propagating part of the spectrum (because of $\text{Re}(k_z)$ and $\text{Re}(k_{2z})$ factors). In other words, the incoherent power spectral coefficients ($\Phi_{s/t,j}^{\text{incoh}}(k_x)$) are only non-zero when $|k_x| \leq k_0$ and $|k_x| < k_2$ for reflected and transmitted power respectively. Thus, the poles at the eigen-mode frequencies (k_x^g) do not appear in the incoherent part. This will happen only in the lossless case when $k_{jz} = \sqrt{k_j^2 - k_x^2}$ is purely imaginary in the evanescent part of the spectrum ($|k_x| > k_j$).

This is not the case with coherent intensities. Coherent intensities are not limited to propagating waves and they are non-zero over the whole spectrum. Therefore, we are faced with the guided modes singularities in the coherent part of the spectrum. In order to capture the total coherent power, theoretically, we need to integrate the coherent power spectral coefficients up to infinity, but in practice,

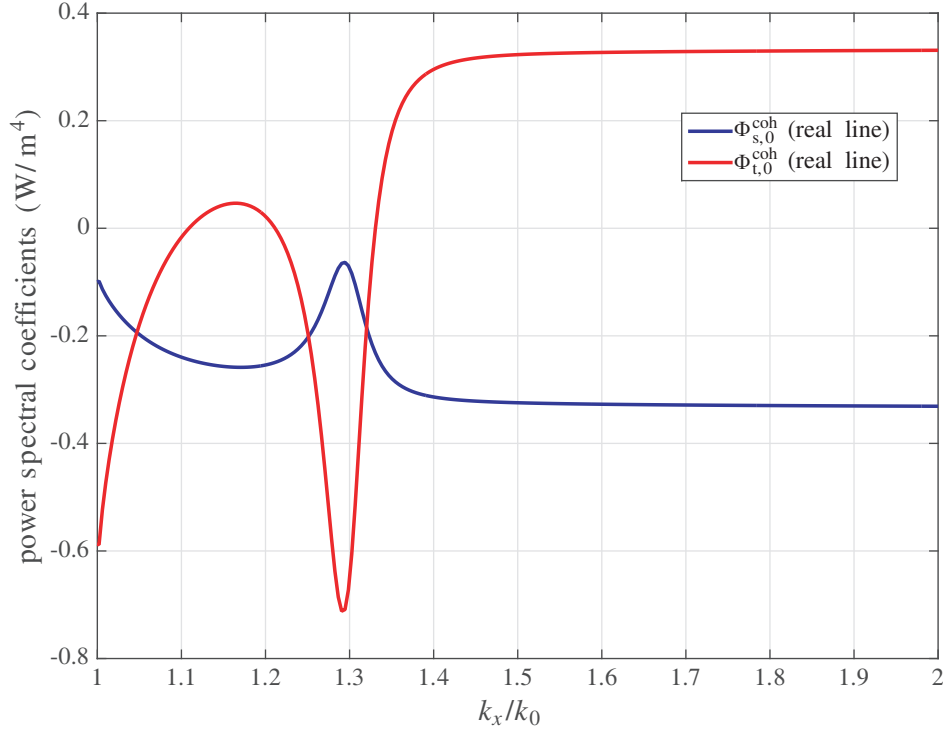


Figure 3. Coherent power spectral density of the first surface, for coherent scattered and transmitted power densities which are evaluated over the real k_x axis. Physical parameters are $\epsilon_0 = \epsilon_0$, $\epsilon_1 = 2\epsilon_0$, $\epsilon_2 = 4\epsilon_0$ and average distance between the surfaces is $0.7\lambda_0$ for the case of normal incidence. Coherent kernel functions $\Phi_{s/t,j}^{\text{coh}}(k_x)$, have no singularity in this case of monotonic dielectric variation.

all of the surfaces are band limited in roughness and we only need to do integration over the spectrum up to some point ($k_{x,\text{max}}$). Here we have two cases; 1 — The power spectral density of the surfaces $W_j(k_x)$, are very band-limited and decay quickly with increasing k_x (very gentle surfaces with large correlation length). In this case we can put an appropriate cutoff for spectral quantities under the integrand ($k_{x,\text{max}} \leq k_0$) and we are not worried about the poles which are always in the evanescent part of the spectrum. 2 — The power spectral densities of the surfaces do not decay rapidly enough (very rough surfaces with fast variations or small correlation length), so it may be necessary to continue integrating the coherent intensities to get a convergent result ($k_{x,\text{max}} > k_0$). In this case the presence of the poles causes serious numerical problems in evaluating the spectral integrals.

Figure 3 plots power spectral coefficients of a two-layer media with dielectric constant of (1, 2, 4) from top to bottom for normal incidence. Note that for the case of monotonic changes in permittivity, the coherent power spectral coefficients are smooth functions of k_x . On the other hand, Fig. 4 plots the coherent power spectral coefficients of the first surface over the real line compared to the corresponding values over the SIP for dielectric constants of (1, 4, 2) from top to bottom. The integrands along the SIP are very gentle, so the integrals can be computed accurately by a relatively coarse numerical integration grid. The price we pay is that we need to increase the integration interval over the SIP to get convergent results. On the other hand, in this way mesh refinement near poles is not necessary, and a uniform grid works over the SIP. Choosing the parameters of the Sommerfeld path accordingly, one can greatly facilitate computation of spectral integrals.

Similarly, Fig. 5 plots the second surface power spectral coefficients over the real line and the SIP.

4.2. SIP Implementation

Figure 6 shows a practical implementation of the SIP in the complex k_x -plane. Here, we need to choose appropriate values for the real cutoff wavenumber $k'_{x,\text{max}}$ and the maximum deviation of path from the

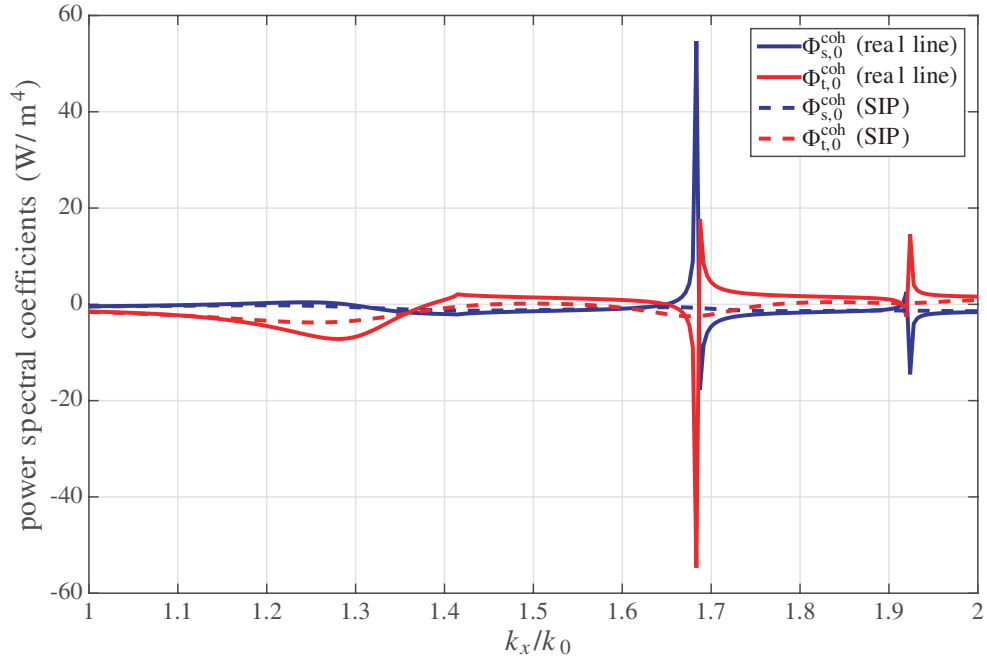


Figure 4. Coherent power spectral density of the first surface, for coherent scattered and transmitted power densities. Physical parameters are given in 4.1. Solid lines are power spectral densities evaluated over the real line which have singularities and cannot be integrated easily, while, dotted lines are the corresponding functions evaluated over the SIP. Variation of integrands is very gentle over the SIP compared to real line.

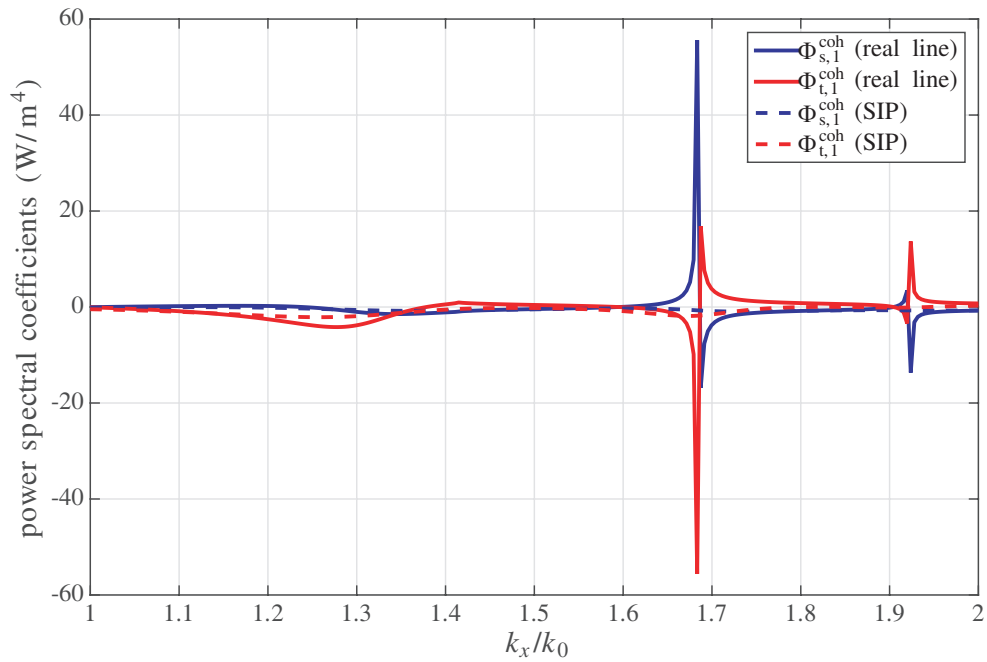


Figure 5. Coherent power spectral density of the second surface, for scattered and transmitted power. Physical parameters are given in 4.1. Solid lines, are power spectral densities evaluated over the real line which have singularities and cannot be integrated easily, while the dotted lines are the corresponding functions evaluated over the SIP. Variation of integrands is very gentle over the SIP compared to the real line.

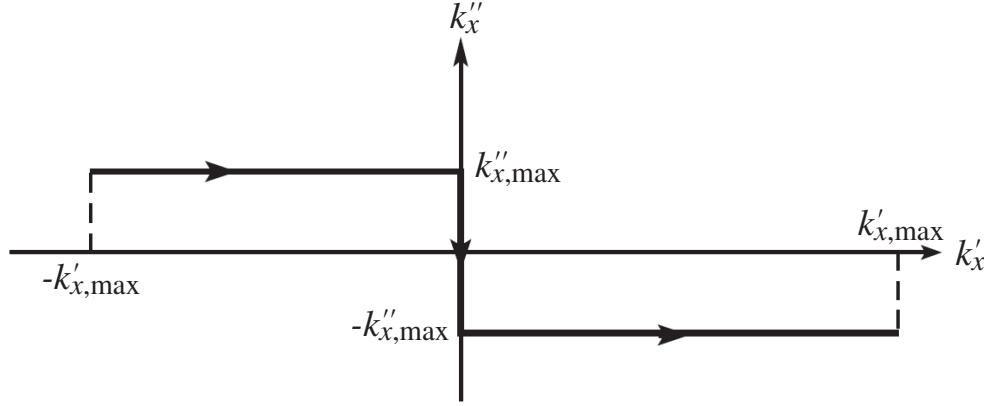


Figure 6. SIP in the complex k_x -plane.

real axis $k'_{x,\max}$. The former is determined by how rapidly the power spectral densities of the surfaces $W_j(k_x)$ attenuate along the k'_x axis. For the latter, in principle we can go up (down) the imaginary axis as high as we want. However, for practical cases taking $k''_{x,\max}$ in the order of $1/d$ (d is the separation between the interfaces) results in smooth kernel functions. Taking $k''_{x,\max}$ very large requires a larger integration domain $k'_{x,\max}$ to obtain convergent results.

We need also to choose the discretization resolution along the real and imaginary axes. Since we do not use the pole locations, we can use a uniform numerical quadrature along the real k_x axis with the grid spacing of $\Delta k'_x$. However For a uniform quadrature, the error term is negligible if

$$\Delta k'_x \ll k''_{x,\max} \quad (67)$$

For the examples in 4.1, we have used $k''_{x,\max} = \frac{0.2}{d}$ and $k'_{x,\max} = 2 \max[k_0, k_1, k_2]$. Also discretization steps along the real axis are chosen to be $\Delta k'_x = 0.2k''_{x,\max}$. The cost for doing the spectral integral in the presence of guided modes using the SIP is not more than required in the regular case (which is the real line spectral integration).

5. COMPARISON WITH THE TRANSLATION OPERATOR (*T*-MATRIX) METHOD

The *T*-Matrix method (also known as extended boundary condition method) is another powerful approach to compute electromagnetic scattering from random surfaces [18]. If the surface of interest is periodic, we can use Floquet's modes as an expansion function for the surface fields. In this way, from the spectral point of view, there are only discrete values of propagation constants for the scattered and transmitted fields. For a sufficiently large period of the surface, the number of propagating Floquet modes becomes so large that it can be considered realistically as a continuous solution of an infinite surface. Thus, for large period surfaces, the *T*-Matrix solution coincides with the solution for an infinite surface problem. Apart from considering the finite period for the surfaces instead of infinite surfaces, the *T*-Matrix method has no approximation. In principle, it works for any surface height, correlation length and any dielectric constants, however, in practice it suffers from numerical issues for some cases (large rms height, small correlation length and high dielectric contrast) and needs to be regularized.

For the first comparison, consider layered media with physical parameters of $\epsilon_0 = \epsilon_0$, $\epsilon_1 = 2\epsilon_0$ and $\epsilon_2 = 4\epsilon_0$ which is the case that cannot support guided modes. Boundary surfaces are considered to be Gaussian correlated, Gaussian random processes with statistical parameters given by $h_{\text{rms}} = 0.03\lambda_0$ and correlation length of $l = \lambda_0$ where λ_0 is the free space wavelength. For the *T*-matrix method we have generated an ensemble of Gaussian periodic random surfaces with Gaussian correlation function. It turns out that for the given physical parameters for the two layered structure, the solution converges after averaging over ≈ 50 realizations. In order to simulate an infinite surface, the period of the surface L is selected as $L = 20\lambda_0$. Each realization of the surface is characterized by 1024 samples (≈ 51 samples/ λ_0) for highly accurate computation of integrals.

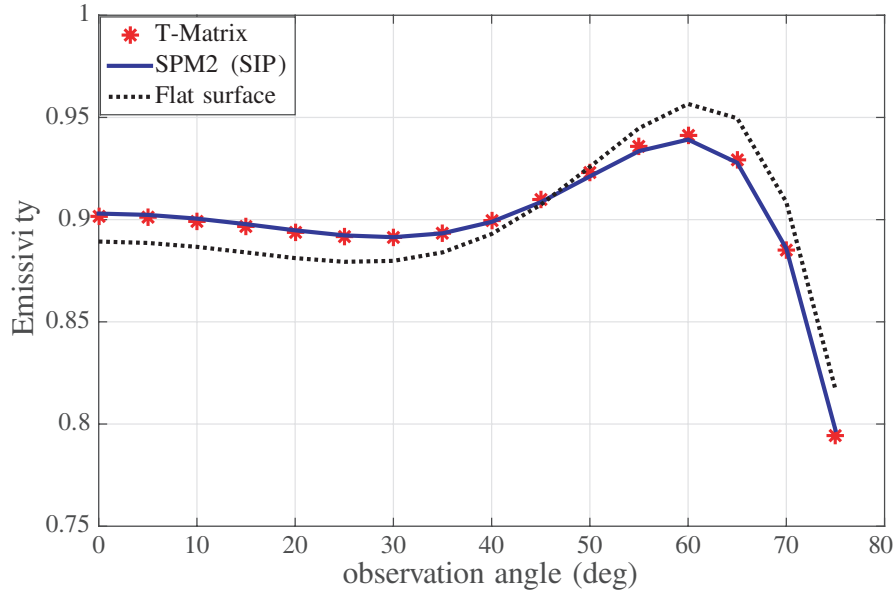


Figure 7. Emissivity of two layer media with permittivities of $\epsilon_0 = \epsilon_0$, $\epsilon_1 = 2\epsilon_0$ and $\epsilon_2 = 4\epsilon_0$ as a function of observation angle. Distance between two half spaces (region 1 thickness) is considered to be $d = 0.7\lambda_0$. For this case where there is no supported guided mode inside the media, SPM2 results coincide with T -Matrix method solution. The dotted line corresponds to the flat boundary limit (presence of roughness smoothes out coherence effect due to reflections from boundaries).

Figure 7 compares emissivity versus observation angle obtained by integrating SPM2 kernels over the SIP with the T -Matrix method solution and the case of zero rms height (flat surfaces) for the regular case where there are no guided modes in the structure (permittivities are $\epsilon_0, 2\epsilon_0, 4\epsilon_0$ from top). In this case, integrating over the SIP for SPM2 kernels gives the same results as the real line integration. For the regular cases (where no mode is supported within the slab), SPM2 kernel functions are smooth and integration over SIP and real line exactly coincide each other. We may conclude that for the regular case the SIP is a valid path of integration and results in correct evaluation of the spectral integrals. Comparison with flat surface emissivity also shows the level of accuracy of SPM2 in including the roughness effect.

As a second example, we consider the case where we encounter guided mode pole in the structure. In order to see how the SIP works in this case, consider the previous configuration with region 1 and 2 interchanged, i.e., $\epsilon_0 = \epsilon_0$, $\epsilon_1 = 4\epsilon_0$ and $\epsilon_2 = 2\epsilon_0$, with other physical parameters kept fixed. Here, this structure can support guided mode, and we have pole singularities in the kernel functions of scattered and transmitted powers.

Figure 8 compares the T -Matrix solution of emissivity versus observation angle, with 1) SPM2 kernel functions integrated over an appropriate SIP, 2) SPM2 kernels integrated over the real line with 100 times finer grid, and 3) zero roughness limit (flat surfaces). Note that in both cases of real line and SIP integration, we did not use the location of the poles. As can be seen from Figs. 7 and 8, the SIP not only works for the regular case, but also is successful in the presence of guided modes, while the real line integral yields erroneous predictions. This indicates that pole singularities can be avoided with only a moderate impact on the integration approach, while continued use of the real line even with very fine resolution remains problematic.

6. EXTENSION TO ARBITRARY NUMBER OF LAYERS

Generalizing the approach to the multi-layer case is straightforward. In this case the integral equations which are related to the extinction of waves in the interior layers are homogeneous [5]. Then, homogeneous integral equations can be cast into recursive ladder propagation matrices for the surface

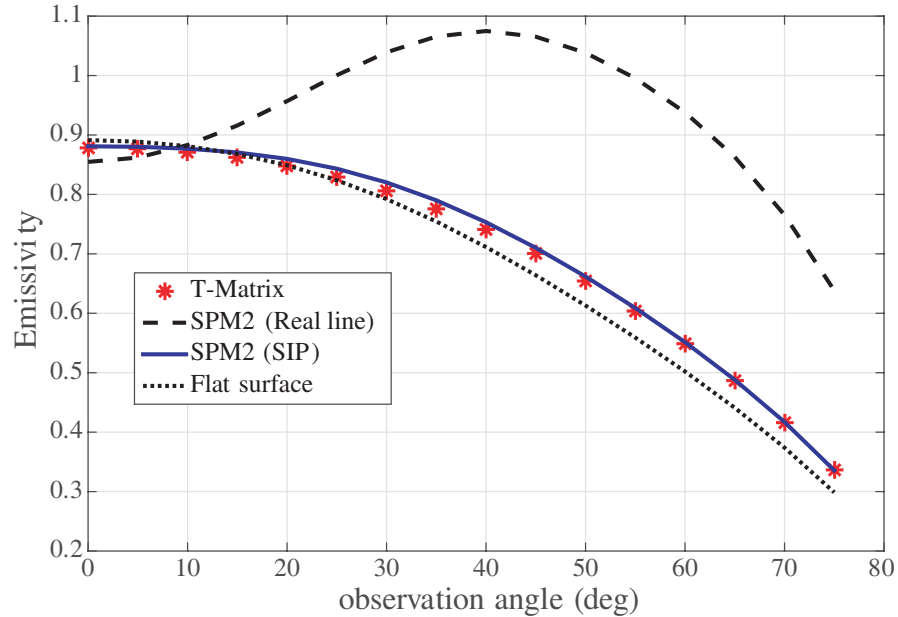


Figure 8. Emissivity of two layer media with permittivities of $\epsilon_0 = \epsilon_0$, $\epsilon_1 = 4\epsilon_0$ and $\epsilon_2 = 2\epsilon_0$ as a function of observation angle. Distance between two half spaces (thickness of region 1) is considered to be $d = 0.7\lambda_0$. For this case where there are supported guided modes inside the media, emissivity obtained by integrating SPM2 power kernels over the SIP are in very good agreement with the *T*-Matrix method solution. Dashed line is corresponding to SPM2 integrated kernel functions over the real line with 100 times finer uniform grid. Real line integration despite 100 times higher computational cost results in non-physical results.

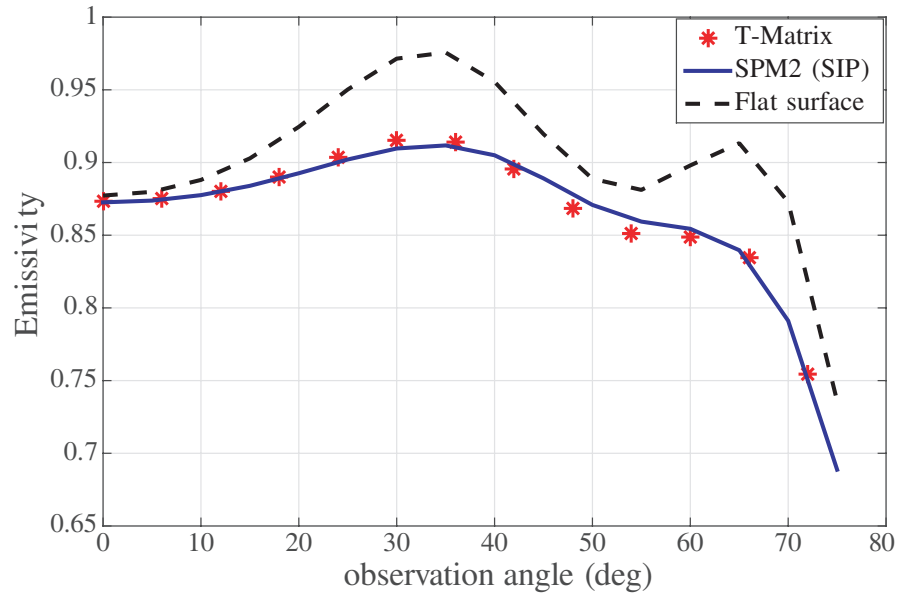


Figure 9. Emissivity of a 5 layer media with permittivities of $(1, 3, 2, 4, 2)\epsilon_0$ from top to bottom, as a function of observation angle. Separations between the mean positions of interfaces are $d_1 = 0.3\lambda_0$, $d_2 = 0.7\lambda_0$ and $d_3 = 0.8\lambda_0$. For this case where there are many supported guided modes inside the media, emissivity obtained by integrating SPM2 power kernels over the SIP are in very good agreement with the *T*-Matrix method solution. Dashed line corresponds to the flat boundaries limit.

fields over the rough boundaries. We do not repeat the procedure here and refer the reader to [5] for a detailed formulation of the problem using ladder operators.

In order to show the validity of the Sommerfeld alternative in multi-mode conditions in a multi-layer medium, consider a stack of 5 media separated by 4 random rough surfaces. We select the permittivity of the layers such that the structure supports guided modes. In this example permittivity of the layers is considered to be $\epsilon_0 = \epsilon_0$, $\epsilon_1 = 3\epsilon_0$, $\epsilon_2 = 2\epsilon_0$, $\epsilon_3 = 4\epsilon_0$ and $\epsilon_4 = 2\epsilon_0$. Separation distances between the mean positions of interfaces are $d_1 = 0.3\lambda_0$, $d_2 = 0.7\lambda_0$ and $d_3 = 0.8\lambda_0$. The T -matrix solution for this case which includes 4 uncorrelated surface processes (all of them Gaussian correlated with rms height of $h = 0.03\lambda_0$ and correlation length of $l = 1\lambda_0$), requiring averaging over a larger number of realizations compared to the 2 layers case. Here, we used an ensemble of 200 realizations (each realization contains 4 uncorrelated surface boundaries) for the emissivity response to converge.

Figure 9 plots the emissivity of the 5-layer structure (with given physical parameters above) obtained by the SIP alternative in comparison with the T -matrix solution and zero rms height (flat surface) limit. The differences between the flat interface case and rough interfaces are larger in this case than just two layers. This also shows that the SIP can capture the impact of multi-layer roughness.

7. CONCLUSION

The application of SPM2 to multi-layer lossless structures (or with small amount of loss) with non-monotonic permittivity profiles results in pole singularities in the integrands of the scattered power densities. It has been shown that we can compute power integrals very accurately at low cost using the Sommerfeld integration path alternative. The validity of the SIP approach for both monotonic and non-monotonic cases has been confirmed by comparing with the T -matrix method.

REFERENCES

1. Tabatabaenejad, A. and M. Moghaddam, "Bistatic scattering from three-dimensional layered rough surfaces," *IEEE Transactions on Geoscience and Remote Sensing*, Vol. 44, No. 8, 2102–2114, 2006.
2. Imperatore, P., A. Iodice, and D. Riccio, "Electromagnetic wave scattering from layered structures with an arbitrary number of rough interfaces," *IEEE Transactions on Geoscience and Remote Sensing*, Vol. 47, No. 4, 1056–1072, 2009.
3. Zamani, H., A. Tavakoli, and M. Dehmollaian, "Second-order perturbative solution of scattering from two rough surfaces with arbitrary dielectric profiles," *IEEE Transactions on Antennas and Propagation*, Vol. 63, No. 12, 5767–5776, 2015.
4. Zamani, H., A. Tavakoli, and M. Dehmollaian, "Scattering from layered rough surfaces: Analytical and numerical investigations," *IEEE Transactions on Geoscience and Remote Sensing*, Vol. 54, No. 6, 3685–3696, 2016.
5. Sanamzadeh, M., L. Tsang, J. T. Johnson, R. J. Burkholder, and S. Tan, "Scattering of electromagnetic waves from 3d multilayer random rough surfaces based on the second-order small perturbation method: Energy conservation, reflectivity, and emissivity," *JOSA A*, Vol. 34, No. 3, 395–409, 2017.
6. Burkholder, R. J., J. T. Johnson, M. Sanamzadeh, L. Tsang, and S. Tan, "Microwave thermal emission characteristics of a two-layer medium with rough interfaces using the second-order small perturbation method," *IEEE Geoscience and Remote Sensing Letters*, Vol. 14, No. 10, 1780–1784, 2017.
7. Wu, C. and X. Zhang, "Second-order perturbative solutions for 3-d electromagnetic radiation and propagation in a layered structure with multilayer rough interfaces," *IEEE Journal of Selected Topics in Applied Earth Observations and Remote Sensing*, Vol. 8, No. 1, 180–194, 2015.
8. Tabatabaenejad, A. and M. Moghaddam, "Study of validity region of small perturbation method for two-layer rough surfaces," *IEEE Geoscience and Remote Sensing Letter*, Vol. 7, No. 2, 319–323, 2010.

9. Johnson, J. T., "Third-order small-perturbation method for scattering from dielectric rough surfaces," *Journal of the Optical Society of America A*, Vol. 16, No. 11, 2720–2736, 1999.
10. Demir, M. A. and J. T. Johnson, "Fourth and higher-order small perturbation solution for scattering from dielectric rough surfaces," *Journal of the Optical Society of America A*, Vol. 20, No. 12, 2330–2337, 2003.
11. Demir, M. A., J. T. Johnson, and T. J. Zajdel, "A study of the fourth-order small perturbation method for scattering from two-layer rough surfaces," *IEEE Transactions on Geoscience and Remote Sensing*, Vol. 50, No. 9, 3374–3382, 2012.
12. Wang, T., L. Tsang, J. T. Johnson, and S. Tan, "Scattering and transmission of waves in multiple random rough surfaces: Energy conservation studies with the second order small perturbation method," *Progress In Electromagnetics Research*, Vol. 157, 120, 2016.
13. Tan, S., M. Aksoy, M. Brogioni, G. Macelloni, M. Durand, K. C. Jezek, T. L. Wang, L. Tsang, J. T. Johnson, M. R. Drinkwater, and L. Brucker, "Physical models of layered polar firn brightness temperatures from 0.5 to 2 GHz," *IEEE Journal of Selected Topics in Applied Earth Observations and Remote Sensing*, Vol. 8, No. 7, 3681–3691, 2015.
14. Sánchez-Gil, J. A., A. A. Maradudin, J. Q. Lu, V. D. Freilikher, M. Pustilnik, and I. Yurkevich, "Scattering of electromagnetic waves from a bounded medium with a random surface," *Phys. Rev. B*, Vol. 50, 15353–15368, Nov. 1994.
15. Freilikher, V., M. Pustilnik, and I. Yurkevich, "Wave scattering from a bounded medium with disorder," *Physics Letters A*, Vol. 193, No. 5, 467–470, 1994.
16. Piegari, A. and F. Flory, *In Optical Thin Films and Coatings: From Materials to Applications*, Woodhead Publishing Elsevier, Cambridge, 2013.
17. Duan, X. and M. Moghaddam, "3-d vector electromagnetic scattering from arbitrary random rough surfaces using stabilized extended boundary condition method for remote sensing of soil moisture," *IEEE Transactions on Geoscience and Remote Sensing*, Vol. 50, No. 1, 87–103, 2011.
18. Tsang, L. and J. A. Kong, *Scattering of Electromagnetic Waves*, Vol. 3: Advanced Topics, Wiley Interscience, 2001.